Available online at www.sciencedirect.com
ScienceDirect
Polymer 47 (2006) 7646–7652
polymer
www.elsevier.com/locate/polymer

Synthesis and characterization of poly(ethyl methacrylate-*co*-methacrylic acid) magnetic particles via miniemulsion polymerization

J.S. Nunes [a], C.L. de Vasconcelos [a], F.A.O. Cabral [b], J.H. de Araújo [b], M.R. Pereira [a], J.L.C. Fonseca [a,*]

[a] *Departamento de Química, Universidade Federal do Rio Grande do Norte, Campus Universitário, Lagoa Nova, Natal, RN 59078-970, Brazil*
[b] *Departamento de Física Teórica e Experimental, Universidade Federal do Rio Grande do Norte, Campus Universitário, Lagoa Nova, Natal, RN 59072-970, Brazil*

Received 18 April 2006; received in revised form 29 August 2006; accepted 2 September 2006
Available online 25 September 2006

Abstract

Magnetic particles are very important systems with potential use in drug delivery systems, ferrofluids, and effluent treatment. In many situations, such as in biomedical applications, it is necessary to cover inorganic magnetic particles with an organic material, such as polymers. In this work, latices based on magnetite covered by poly(ethyl methacrylate-*co*-methacrylic acid) were obtained via miniemulsion polymerization. The resultant latices had particles in the nanometric range and presented a pronounced superparamagnetic behavior.

Keywords: Poly(ethyl methacrylate); Magnetite; Magnetic latex

1. Introduction

Ferrofluids, or magnetic fluids, are stable dispersions of ultrafine magnetic particles (sometimes encapsulated magnetic particles) in an aqueous or organic continuous phase [1]. The stability of these dispersions is obtained using a surfactant which prevents flocculation, followed by sedimentation [2]. Ideally, these particles should remain uniformly dispersed within the continuous phase, even when submitted to magnetic fields [3].

Magnetic polymeric particles usually are the result of covering of magnetic iron oxide (Fe_3O_4) via physical interactions with macromolecules as well as chemical reactions between the inorganic oxide surface and the organic material [4]. Such particles are well-known materials and have been widely studied due to their applications in diverse areas, such as biology, medicine and environmental remediation [5]. These applications involve separation of enzymes and proteins, purification of nucleic acids [6], techniques of magnetic resonance imaging for cancer diagnostics [7] and cancer therapy through drug carriers that are magnetically controlled [8,9]. Hiergeist et al. have developed ferrofluids with potential use as magnetic materials for hyperthermia of biological tissue, with the goal of tumor therapy [10]. Another important example is the removal of toxic industrial waste by magnetic particles [11,12].

Different kinds of magnetic particles have been produced with both natural and synthetic polymers with the objective of incorporating groups on their surface, or modifying it, in order to carry out selective separations [13]. The incorporation of inorganic particles to polymers results in materials of higher mechanical strength [14,15], thermal stability [16] and superior optical [17], magnetic and electric properties [18]. Particles of nanometric dimensions (10–500 nm), such as nanocrystals [19], present high surface area, promoting a better dispersion within the polymer matrix, allowing one to obtain interesting nanoparticulated materials with unique dimensional quantum effects, transport and magnetic properties.

* Corresponding author. Tel.: +55 84 3215 2828x215; fax: +55 84 3221 9224.
E-mail address: jlcfonseca@uol.com.br (J.L.C. Fonseca).

0032-3861/$ - see front matter © 2006 Elsevier Ltd. All rights reserved.
doi:10.1016/j.polymer.2006.09.006

The controlled polymer synthesis in the presence of inorganic nanoparticles results in nanocomposite dispersions that have polymer matrices with very specific properties, combined with low production costs [20], so that surface-related properties of these hybrid materials are chiefly determined by the polymer matrix [21]. These hybrid materials can be used in biomedical applications, as Španová et al. have shown using dispersion polymerization for obtaining magnetic microparticles for separation and identification of microbial species [22].

The process of miniemulsion polymerization can be used for an efficient covering of water-insoluble materials with hydrophobic polymers, in order to obtain hybrid materials that are homogeneous both in particle size and inorganic material content [23,24]. Monomer miniemulsions are the result of the critical stabilization of monomer droplets (in the form of micelles, with size ranging from 50 to 500 nm), prepared by shearing of a system containing monomer, water, surfactant and a hydrophobic substance [25]. Polymerization reactions, when carefully prepared, result in latex particles of size similar to the initial size of the monomer droplets [26]. The process involves an initiator soluble in the continuous phase, a surfactant and monomers insoluble (or poorly soluble) in water, which are in the form of droplets stabilized by the surfactant. The polymerization reactions preferentially occur on growing particles and in micelles of surfactant, but may partially occur in the continuous phase. The main advantage of emulsion-based polymerization methods consists in the control on the molecular weight and molecular weight distribution, using parameters such as the initiator and/or surfactant concentrations [27,28].

The reduced chemical affinity between the inorganic particles (of hydrophilic nature) and the monomer (predominantly hydrophobic) is an important aspect to be considered in the preparation of magnetic particles. The compatibility of the particles with the polymeric matrix can be improved by the surface chemical modification of the particles [29]. To do so, normally use is made of an agent which promotes chemical compatibilization via hydrogen bonding, electrostatic interactions or covalent bonds within the inorganic/organic interface. Oleic acid has been widely used to disperse magnetite in styrene, the resultant dispersion being polymerized in miniemulsion, so that dispersed polystyrene particles (with magnetite dispersed within the polymer matrix) have been obtained [30]. The substitution of surfactant by polymers may avoid aggregation of inorganic particles but, on the other hand, may provoke bridging flocculation [20]. Using these techniques, Liu et al. have modified magnetite, obtaining functionalized magnetic nanospheres via miniemulsion polymerization with methyl methacrylate and divinylbenzene, as a crosslinking agent [31]; Pich et al. have obtained magnetic hybrid latices using surfactant-free emulsion copolymerization of styrene and acetoacetoxyethyl methacrylate onto iron oxide nanoparticles [32].

In this work, the synthesis of magnetic latices of poly(ethyl methacrylate-*co*-methacrylic acid) and magnetite is prepared via miniemulsion polymerization, using oleic acid as the stabilizing agent for magnetite, sodium dodecyl sulfate as the surfactant and 2,2′-azobis(isobutyronitrile) as the initiator. As far as we know, it is the first time ethyl methacrylate is used for this purpose. The use of this monomer is interesting because of the glass transition temperature of the homopolymer, $T_g = 65\ ^\circ C$, so that one can obtain films with good mechanical strength and flexibility. The resultant latices are characterized in terms of their physicochemical and magnetic properties.

2. Experimental

Ferrous sulfate heptahydrate – $FeSO_4 \cdot 7H_2O$ (PA, Labsynth, Brazil), ferric sulfate nonahydrate – $Fe_2(SO_4)_3 \cdot 9H_2O$ (PA, Synth, Brazil), sodium dodecyl sulfate (SDS) – $C_{12}H_{15}SO_4Na$ (PA, Synth, Brazil), ammonium hydroxide – NH_4OH (30 wt%, PA, CRQ, Brazil), ethanol – C_2H_5OH (PA, Synth, Brazil), oleic acid (OA) – $C_{18}H_{34}O_2$ (Vetec, Brazil), 2,2′-azobis(isobutyronitrile) (AIBN) (Aldrich, USA), and methacrylic acid (MAA) (Aldrich, USA) were used as received. Ethyl methacrylate (EMA) (Unigel, Brazil) was washed with 5 wt% aqueous NaOH prior to use, in order to eliminate inhibitor (methylhydroquinone). The same procedure was not used for MAA due to its solubility in water as well as to the fact that it was used in a mass percentage of 1%, in terms of monomer composition. Bidistilled water was used in all the experiments.

2.1. Synthesis of magnetite nanoparticles

Magnetite nanoparticles used in this work were prepared via the method of chemical co-precipitation [33]. In this method magnetite is obtained as a result of the co-precipitation of ions Fe^{2+} and Fe^{3+} by the addition of NH_4OH to a solution containing the mentioned ions at a molar ratio $Fe^{2+}/Fe^{3+} = 1/2$, until the resultant dispersion reaches a pH around 11, at room temperature. The process of synthesis of magnetite can be described according to Eq. (1):

$$Fe^{2+} + 2Fe^{3+} + 8OH^- \rightarrow Fe_3O_4 + 4H_2O \quad (1)$$

It has been repeatedly reported that particles synthesized using this method may be as small as 9 nm [34], and are very sensitive to oxidation by the oxygen from air, forming $Fe(OH)_3$, as shown by Eq. (2), or a maghemite (γ-Fe_2O_3) according to Eq. (3):

$$Fe_3O_4 + \frac{1}{4}O_2 + \frac{9}{2}H_2O \rightarrow 3Fe(OH)_3 \quad (2)$$

$$2Fe_3O_4 + \frac{1}{2}O_2 \rightarrow 3\gamma\text{-}Fe_2O_3 \quad (3)$$

The occurrence of hematite phase (α-Fe_2O_3) is more difficult than the maghemite one, only occurring under thermal dehydration conditions [5]. Additionally, small amounts of dissolved O_2 in water may oxidize Fe^{2+} ions to Fe^{3+}as shown by Eq. (4), also resulting in the formation of $Fe(OH)_3$ or γ-Fe_2O_3, as shown, respectively, by Eqs. (5) and (6):

$$Fe^{2+} + \frac{1}{2}H_2O + \frac{1}{4}O_2 \rightarrow Fe^{3+} + OH^- \quad (4)$$

$$Fe^{3+} + 3OH^- \rightarrow Fe(OH)_3 \quad (5)$$

$$2Fe^{3+} + 6OH^- \rightarrow \gamma\text{-}Fe_2O_3 + 3H_2O \quad (6)$$

2.2. Hydrophobization of magnetite nanoparticles

The magnetite nanoparticles were magnetically separated from the supernatant and re-dispersed in water for several times, until the continuous phase pH reached a value around 7. A final magnetic separation was carried out and a given amount of oleic acid was added to the particles, in order to obtain magnetite with hydrophobic surface. The hydrophobization of the magnetite particles could be characterized by the complete segregation of these particles from the water phase, forming a black greasy non-polar phase. Two different types of hydrophobized magnetites were obtained: in one, it was added a mass of oleic acid equal to the mass of magnetite; in other, the mass of oleic acid was 50% of the mass of magnetite.

2.3. Polymerization

A miniemulsion of ethyl methacrylate and methacrylic acid was prepared through the addition of 20.38 g of EMA and 0.206 g of MAA to a given amount of hydrophobized magnetite nanoparticles. The mixture was immersed in an ice bath, which was immersed in an ultrasonic bath (Transsonic 460, Elma, Germany) under mechanical stirring for 20 min. Following, the mixture (monomers and magnetite) was added to a solution of 0.206 g of SDS in 225 g of water and submitted again to ultrasonication in an ice bath, under mechanical stirring, for more 20 min. In order to initiate polymerization, 0.103 g of AIBN was added to the system and the temperature was increased to 75–80 °C. The system was maintained at this temperature, under mechanical stirring, for 3 h.

Three types of latex were synthesized. One had a magnetite/monomer mass ratio of 10% ($w_{Fe_3O_4/monomer} = 0.1$) and a mass ratio of OA/magnetite of 1 ($w_{OA/Fe_3O_4} = 1$); another one with the same magnetite content and a lower OA/magnetite mass ratio ($w_{OA/Fe_3O_4} = 0.5$); and the third one had $w_{Fe_3O_4/monomer} = 0.2$ and $w_{OA/Fe_3O_4} = 1$. These latices were respectively named Latex I, Latex II, and Latex III, their compositions being summarized in Table 1. Fig. 1 presents a scheme which depicts all the process of obtaining the polymer-coated magnetite particles.

Table 1
Compositions of latices I–III: w_{OA/Fe_3O_4} is the (oleic acid)/magnetite mass ratio and $w_{Fe_3O_4/monomer}$ is the magnetite/monomer mass ratio

Latex	w_{OA/Fe_3O_4}	$w_{Fe_3O_4/monomer}$
I	1	0.1
II	0.5	0.1
III	1	0.2

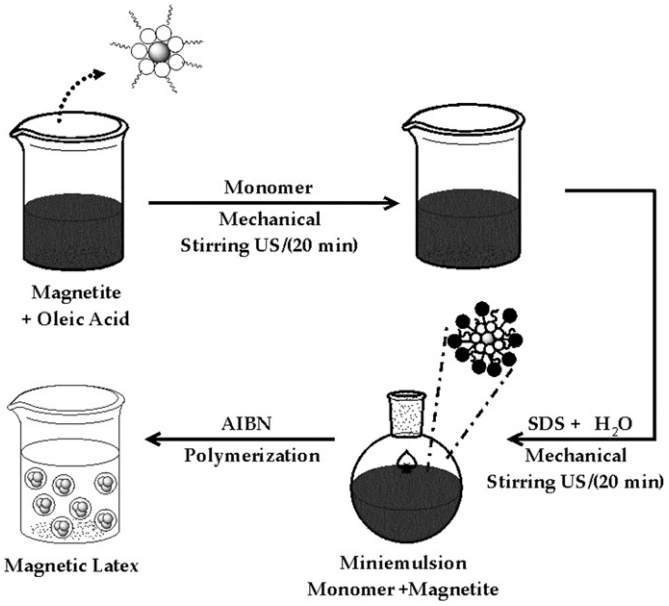

Fig. 1. Scheme representing magnetic latex synthesis.

2.4. Latex coagulation

The latices were coagulated by the addition of ethanol to the dispersions. Excess of ethanol was used in order to wash the particles to remove unreacted species from the polymer. After drying in vacuum for 12 h, the resultant aggregates were grounded, resulting in brownish particles, with a color intensity dependent on the amount of inorganic material used in the composition of each latex.

2.5. Particle characterization

The crystalline phase of the latices was identified by X-ray diffraction, using Cu Kα radiation at 30 kV/30 mA from a Shimadzu X-ray diffractometer, model Lab-X XRD 60000, with a scan angle 2θ ranging from 10 to 80 °C, in intervals of 0.02° and a time of 0.60 s between each interval. In order to obtain the size of the magnetite crystallites of pure magnetite and the magnetite dispersed within the polymeric matrix the results obtained from XRD were refined using Rietveld method. To carry out this work the software MAUD 2.038, developed by Luca Lutterotti, was used with the diffraction data as described in the literature [35].

Fourier transform infrared (FTIR) spectroscopy was carried out using KBr pellets for magnetite and coagulated latices. The equipment used in this characterization was an FTIR spectrometer Nicolet Nexus 470. The operational parameters in these analysis were: wavelength range, 4000–400 cm^{-1}; resolution, 4 cm^{-1}; number of scans, 32.

Scanning electron microscopy (SEM) images of the coagulated particles were obtained using a Phillips XL30 electron microscope (filament, tungsten; voltage 25.0 kV; detector, secondary electrons). Prior to the analysis, all samples were metalized with gold.

2.6. Magnetization curves

Magnetization measurements were carried out using a vibrating sample magnetometer (VSM) to study magnetic properties of the magnetic nanoparticles in magnetic fields up to 12 kOe. In this experiment the sample is subjected to a vertical sinusoidal magnetic field and the variation of the magnetic flow around the sample induces an electrical signal that, after further processing, is sent to a data acquisition device plugged to a computer, which converts it to magnetization. A more detailed description of this equipment may be found in a paper already published by some of the authors of the present work [36].

3. Results and discussion

Magnetite resulting from the co-precipitation method was dense, black, and strongly magnetic (a simple loudspeaker magnet was able to attract the particles). The latices with incorporated magnetite were stable for more than four months and the coagulated particles also had markedly magnetic properties: particles from the latices presented brownish color, depending on the amount of magnetite present in them – the color ranged from black, for pure magnetite, to white, pure poly(ethyl methacrylate-*co*-methacrylic acid).

3.1. Scanning electron microscopy (SEM)

Fig. 2 shows a micrograph of magnetite and of a magnetic latex after coagulation (Latex II). A comparison of the magnetite micrograph with the one related to the latex with dispersed magnetite suggests that magnetite was dispersed within the polymeric matrix. The other latices presented a morphology very similar to the one shown in this figure: coagulated particles comprised of clusters of particles with linear dimensions below 500 nm. As a consequence, these particles could be considered to be within the nanometric range. The morphology of these nanoparticles exhibited spherical forms with considerable polydispersion. Regarding size distribution, the nature of our particles made them much more difficult to analyze, as it has been done by the excellent works of Liu et al. [31] and Pich et al. [32] with divinylbenzene crosslinked poly(methyl methacrylate) particles and poly(styrene/methacrylate) copolymers, respectively. When polystyrene or poly(methyl methacrylate) is used as the polymer matrix for magnetite, its non-polar nature (in the case of polystyrene) and high T_g (both in the case of polystyrene and PMMA, mainly if it is crosslinked with divinylbenzene) favors the occurrence of well-separated particles. In our case, apart from ethyl methacrylate being more polar than styrene and the resulting uncrosslinked polymer being softer than PMAA, there is also the presence of carboxyl groups from the methacrylic acid, which makes particle aggregation (during provoked latex destabilization) unavoidable.

3.2. X-ray diffraction (XRD)

Fig. 3 shows the results of X-ray diffraction for the magnetite particles and the synthesized latices. The results show the

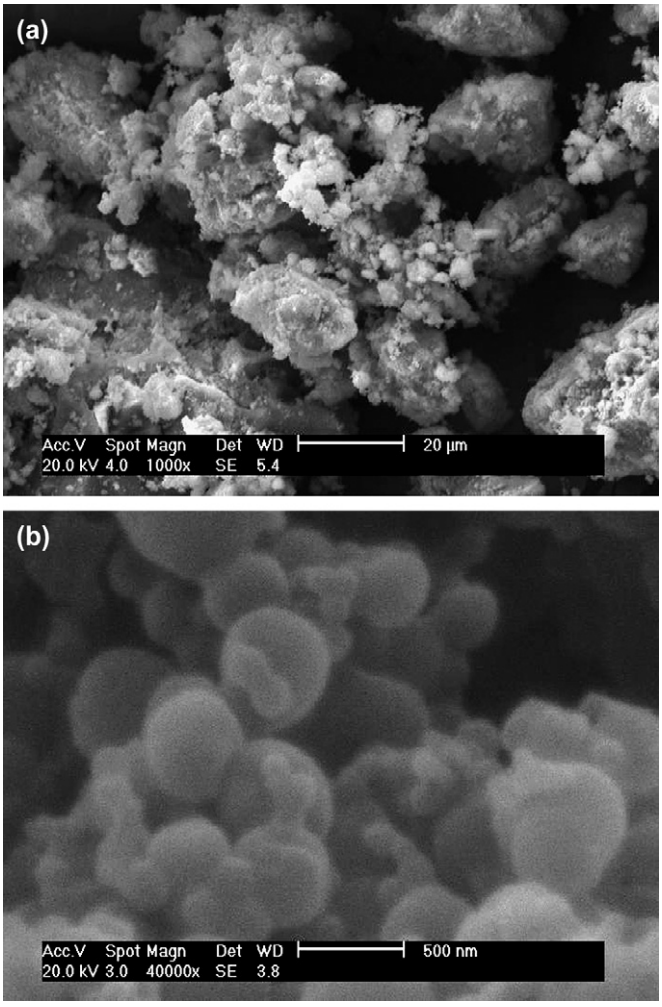

Fig. 2. SEM micrograph of (a) agglomerated magnetite (1000×) and (b) latex II coagulated particles (40,000×).

spinel phase structure of magnetite and are in agreement with the XRD standard [37] for the magnetite particles (Table 2). The results also show that magnetite is the dominant phase in the coagulated latices, though small amounts of maghemite may be formed during the process of co-precipitation and polymerization, as pointed out in Section 2.1. Maghemite is brown, while magnetite is black; however, when present in traces, it is very difficult to distinguish maghemite from magnetite only by its color. This task becomes impossible if we have in mind that the presence of PEMA *per se* gives a brownish tone to the particles.

The structure refinement using the Rietveld method yielded the results shown in Table 3. One can see that crystallite sizes were around 13–15 nm, independent of magnetite being dispersed within the polymethacrylate matrix or not. The average size of the crystallite was in the same range of the optimum values of 9 nm reported in the literature [34].

3.3. Infrared spectroscopy

Fig. 4 shows the spectra of pure PEMA, latices I–III, and magnetite (in order to confirm the presence of magnetite in

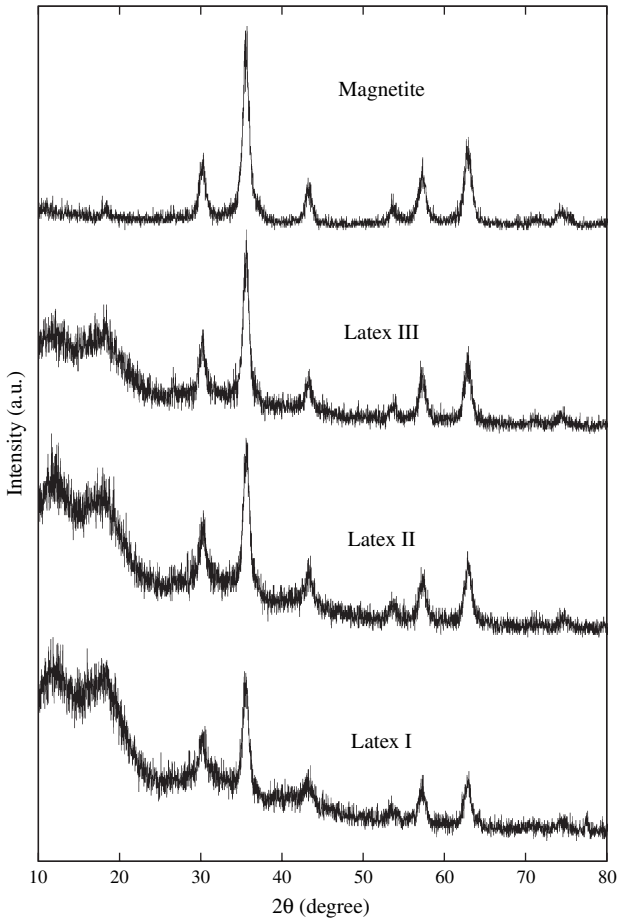

Fig. 3. Diffractogram of magnetite and latices obtained in this work.

the synthesized latices). The presence of magnetite in the latices is characterized by two absorption bands at 632 and 585 cm^{-1}. These bands result from the split of the ν_1 band at 570 cm^{-1}, which corresponds to the Fe−O bond in magnetite; additionally, a band observed at 421 cm^{-1}, corresponding to the ν_2 band of the Fe−O linkage in magnetite (as a matter of fact, this value is due to a shift from its original value of 375 cm^{-1}) [5,37].

All the other bands found in the infrared spectra are characteristic of the acrylic polymer [28,38]. One can see that bands of moderate intensity related to methyl and methylene absorptions are observed in the spectra (at 2957 and 2874 cm^{-1}). Bending of methyl groups is observed at 1481 cm^{-1} (CH_3 and CH_2 bending), 1448 cm^{-1} (asymmetric bending of CH_3) and 1388 cm^{-1} (symmetric bending of CH_3). The intense bands at 1727 and 1270 cm^{-1} are due to the absorption of the highly polar carboxyl groups present in the polymer [39], which presents axial deformation mode of C═O at 1727 cm^{-1}, while the band at 1270 cm^{-1} is attributed to the axial deformation of the C−O bond. The presence of hydroxyl groups is very evident in the spectra of the coagulated latices from the absorption at 3433 cm^{-1}. These bands probably come from absorbed water in the particles.

Table 2
X-ray diffraction data of synthesized magnetite particles

2θ (exp)	d (exp)	hkl	d (Fe_3O_4) [37]	I/I_0
18.5°	4.80	(111)	4.85	5
30.2°	2.95	(220)	2.97	31
35.6°	2.52	(311)	2.53	100
43.2°	2.09	(400)	2.10	20
57.2°	1.61	(511)	1.62	27
62.8°	1.48	(440)	1.48	42

2θ is the angle of incidence, d (exp) is the calculated interplanar spacing between the hkl diffracting planes, d (Fe_3O_4) is the standard value for magnetite, and I/I_0 is the ratio between the intensity of a particular peak and the intensity of the peak at $2\theta = 35.6°$.

Table 3
Magnetite crystallite sizes, obtained using the Rietveld method

Sample	Crystallite size (nm)
Pure magnetite	13
Latex I	15
Latex II	13
Latex III	15

3.4. Magnetization

The magnetization curves for the Fe_3O_4 nanoparticles and the three kinds of magnetic latices are shown in Figs. 5 and 6. From the obtained cycles of magnetization (M, as a function

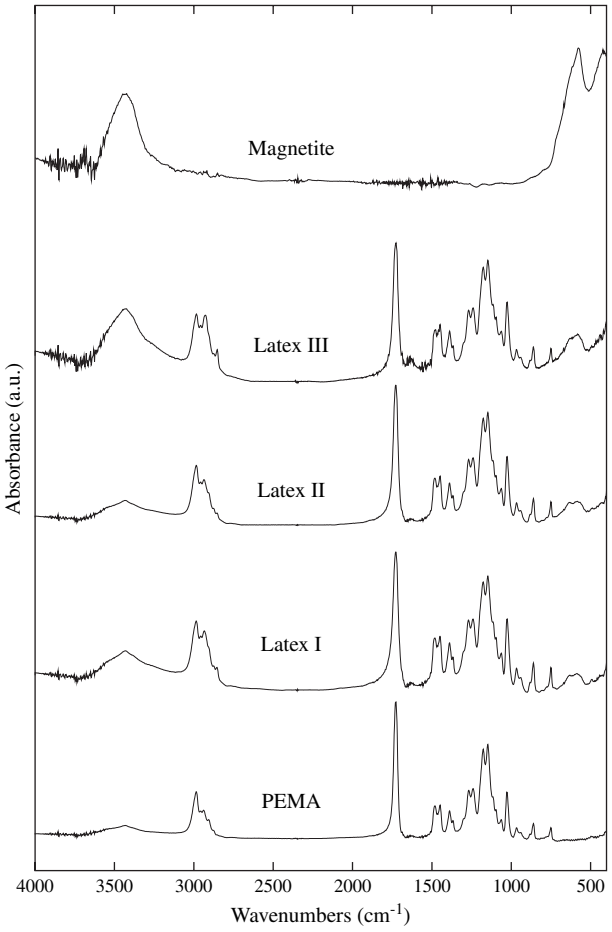

Fig. 4. Infrared spectra of magnetite and the latex particles obtained in this work.

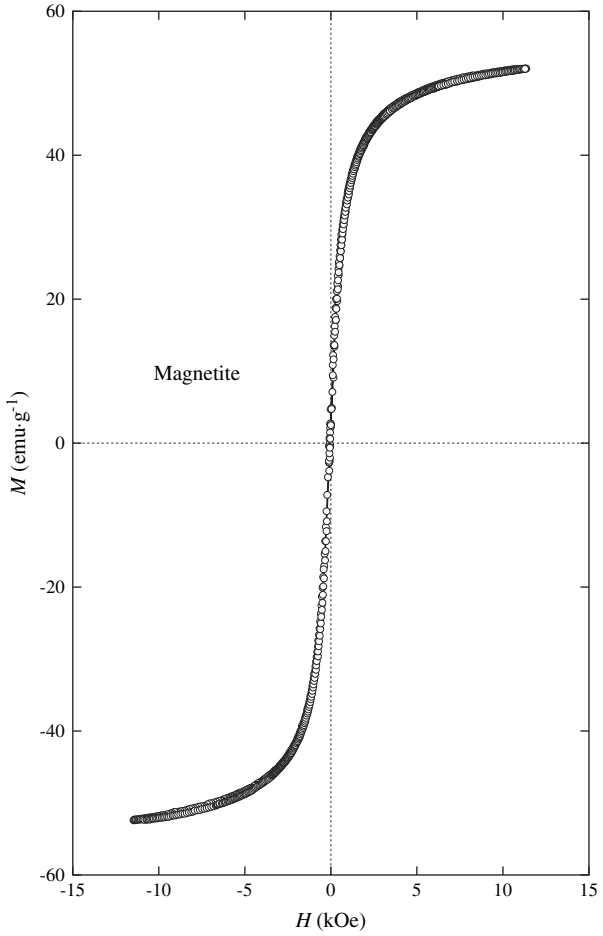

Fig. 5. Magnetization, M, as a function of magnetic field, H, for the magnetite particles obtained in this work.

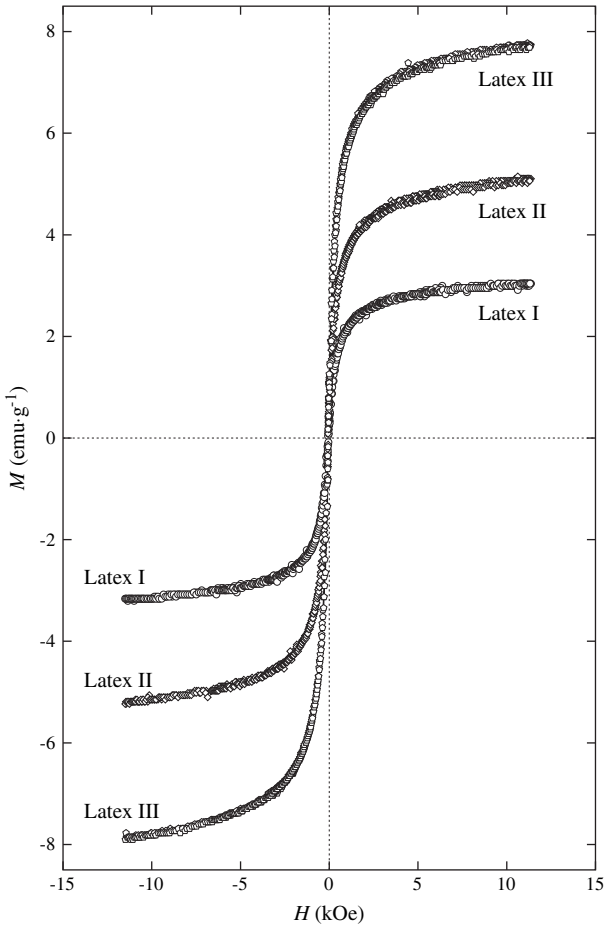

Fig. 6. Magnetization, M, as a function of magnetic field, H, for the latex particles obtained in this work.

of applied magnetic field, H), the following parameters were determined for the particles:

- The saturation magnetization, M_S, which is the maximum magnetization obtained for a given sample. At the value of $M = M_S$ the domains are fully aligned to the field H, resulting in a constant value of magnetization, independent of the value of H.
- The coercivity, H_C, which are the values of H at the points in which the magnetization curve intercepts the magnetic field axis.
- The remanent magnetization, M_R, which are the values of M at the points in which the magnetization curve intercepts the magnetization axis.

The values of H_C and M_R may be used as a quantification of the occurrence of magnetic hysteresis (the lower these parameters are, the lower the hysteresis effects are). A superparamagnetic behavior is characterized by a hysteresis cycle with low values of H_C and M_R.

As one can see in Table 4, in the case of magnetite, a value of saturation magnetization of 52 emu g^{-1} was determined (as a matter of fact an asymptotic value was not reached within the used range of magnetic field, so that M_S must have a slightly higher value). It is a low value, compared to the value of 92 emu g^{-1}, reported for bulk magnetite [40,41]. Some authors have correlated the decrease in M_S for magnetite nanoparticles (compared to bulk magnetite) to surface processes bound to the nanometric dimensions of the particles [42]. Indeed, one can find values of M_S already reported in the literature, using the method of co-precipitation method [7,43], within the same range found in this work. Finally, many of the magnetization cycles are obtained at temperatures around 5–10 K, while ours were carried out at room temperature: it has been shown that, for nanosolids, saturation magnetization dramatically decreases at room temperature [44]. Both remanent magnetization and coercivity were small, suggesting that the nanoparticles were superparamagnetic [45].

Table 4
Magnetic properties of the nanoparticles

Sample	M_S (emu g^{-1})	M_R (emu g^{-1})	H_C (kOe)
Magnetite	52	2.3	0.04
Latex I	3.0	0.19	0.04
Latex II	5.1	0.46	0.03
Latex III	7.7	1.0	0.03

M_S is the saturation magnetization, M_R is the remanent magnetization, and H_C is the coercivity.

Superparamagnetism, that is, responsiveness to an applied magnetic field without permanent magnetization, is critical for magnetic bioseparation because it ensures repeated use of magnetic adsorbents and efficient product elution [46]. In the case of latices I–III, Fig. 6 also reflects superparamagnetic behavior, due to the low values of M_R and H_C, as also shown in Table 4.

4. Conclusions

Miniemulsion polymerization was successfully used in the preparation of magnetic latices for polymer covering of primary magnetite nanoparticles. Magnetite particles resisted to the conditions used in the miniemulsion polymerization: indeed, oleic acid coverage seemed to increase the stability of magnetite particles toward oxidation during sonication/polymerization. The linear dimensions of the synthesized particles were in the nanometric range ($\leq$500 nm) and saturation magnetization increased with increasing of magnetite content. The resultant particles had a superparamagnetic nature, so that they may be potentially used for magnetic (bio)separation processes.

Acknowledgments

The authors thank Brazil's Conselho Nacional de Desenvolvimento Científico e Tecnológico (CNPq), Ministério da Ciência e Tecnologia (MCT), Fundação Coordenação de Aperfeiçoamento de Pessoal de Nível Superior (CAPES), CTPETRO, FINEP, and Pró-Reitoria de Pesquisa da Universidade Federal do Rio Grande do Norte (PROPESQ-UFRN) for financial support during the course of this work. The authors also thank Ms Debora A. Nunes and Unigel for kindly supplying EMA used in this work.

References

[1] Horng HE, Hong CY, Yang SY, Yang HC. J Phys Chem Solids 2001;62:1749–64.
[2] Avdeev MV, Aksenov VL, Balasoiu M, Garamus VM, Schreyer A, Török G, et al. J Colloid Interface Sci 2006;295:100–7.
[3] Ramírez LP, Landfester K. Macromol Chem Phys 2003;204:22–31.
[4] Raj K, Moskowitz B, Casciari R. J Magn Magn Mater 1995;149:174–80.
[5] Yamaura M, Camilo RL, Sampaio LC, Macedo MA, Nakamura M, Toma HE. J Magn Magn Mater 2004;279:210–7.
[6] Deng Y, Wang L, Yang W, Fu S, Elaïssari A. J Magn Magn Mater 2003;257:69–78.
[7] Kim EH, Lee HS, Kwak BK, Kim BK. J Magn Magn Mater 2005;289:328–30.
[8] Alexiou C, Schmidt A, Klein R, Hulin P, Bergemann C, Arnold W. J Magn Magn Mater 2002;252:363–6.
[9] Kohler N, Sun C, Wang J, Zhang MQ. Langmuir 2005;21:8858–64.
[10] Hiergeist R, Andrä W, Buske N, Hergt R, Hilger I, Richter U, et al. J Magn Magn Mater 1999;201:420–2.
[11] Liu QX, Xu ZH. J Appl Phys 1996;79:4702–4.
[12] Ambashta RD, Wattal PK, Singh S, Bahadur D. J Magn Magn Mater 2003;267:335–40.
[13] Zheng W, Gao F, Gu H. J Magn Magn Mater 2005;288:403–10.
[14] Nunes RCR, Fonseca JLC, Pereira MR. Polym Test 2000;19:93–103.
[15] Nunes RCR, Pereira RA, Fonseca JLC, Pereira MR. Polym Test 2001;20:707–12.
[16] Qiu WL, Luo YJ, Chen FT, Duo YQ, Tan HM. Polymer 2003;44:5821–6.
[17] Khrenov V, Klapper M, Koch M, Mullen K. Macromol Chem Phys 2005;206:95–101.
[18] Zhang ZM, Wan MX, Wei Y. Nanotechnology 2005;16:2827–32.
[19] Sargent EH. Adv Mater 2005;17:515–22.
[20] Esteves ACC, Barros-Timmons A, Trindade T. Quím Nova 2004;27:798–806.
[21] Sinsawat A, Anderson KL, Vaia RA, Farmer BL. J Polym Sci Part B Polym Phys 2003;41:3272–84.
[22] Španová A, Horák D, Soudková E, Rittich B. J Chromatogr B 2004;800:27–32.
[23] Castelvetro V, de Vita C. Adv Colloid Interface Sci 2004;108:167–85.
[24] Csetneki I, Faix MK, Szilagyi A, Kovacs AL, Nemeth Z, Zrinyi M. J Polym Sci Part A Polym Chem 2004;42:4802–8.
[25] Bouanani F, Bendedouch D, Maitre C, Teixeira J, Hemery P. Polym Bull 2005;55:429–36.
[26] Asua JM. Prog Polym Sci 2002;27:1283–346.
[27] Woo BH, Jiang G, Jo YW. Pharm Res 2001;18:1600–6.
[28] Nunes JS, de Vasconcelos CL, Dantas TNC, Pereira MR, Fonseca JLC. Colloids Surf A 2006;275:148–52.
[29] Kunze C, Freier T, Helwig E, Sandner B, Reif D, Wutzler A, et al. Biomaterials 2003;24:967–74.
[30] Hoffmann D, Landfester K, Antonietti M. Magnetohydrodynamics 2001;37:217–21.
[31] Liu XQ, Guan YP, Ma ZY, Liu HZ. Langmuir 2005;20:10278–82.
[32] Pich A, Bhattacharya S, Ghosh A, Adler HJ. Polymer 2005;46:4596–603.
[33] Barnakov YA, Scott BL, Golub V, Kelly L, Reddy V, Stokes KL. J Phys Chem Solids 2004;65:1005–10.
[34] Cheng FY, Su CH, Yang YS, Yeh CS, Tsai CY, Wu CL, et al. Biomaterials 2005;26:729–38.
[35] Sahu P. Intermetallics 2006;14:180–8.
[36] Soares JM, de Araújo JH, Cabral FAO, Dumelow T, Machado FLA, de Araújo AEP. Appl Phys Lett 2002;80:2532–4.
[37] Ma M, Zhang Y, Yu W, Shen HY, Zhang HQ, Gu N. Colloids Surf A 2003;212:219–26.
[38] de Medeiros DWO, da Trindade Neto CG, dos Santos DES, Pavinatto FJ, dos Santos DS, Oliveira Jr ON, et al. J Dispersion Sci Technol 2005;26:267–73.
[39] Stuart B, George W, McIntyre PS. Modern infrared spectroscopy. Chichester: John Wiley & Sons; 1996. p. 106.
[40] Dresco P, Zaitsev VS, Gambino RJ, Chu B. Langmuir 1998;15:1945–51.
[41] Lin CR, Chu YM, Wang SC. Mater Lett 2004;60:447–50.
[42] Long Y, Chen Z, Duvail JL, Zhang Z, Wan M. Physica B 2005;370:121–300.
[43] Peng ZG, Hidajat K, Uddin MS. J Colloid Interface Sci 2004;271:277–83.
[44] Zhong WH, Sun CQ, Li S, Bai H, Jiang E. Acta Mater 2005;53:3207–14.
[45] Mooney KE, Nelson JA, Wagner MJ. Chem Mater 2004;16:3155–61.
[46] Ma Z, Guan Y, Liu H. J Polym Sci Part A Polym Chem 2005;43:3433–9.